Bottomonium transport in *p*-Pb and Pb-Pb collisions at energies available at the CERN Large Hadron Collider

Baoyi Chen* and Bo Tong
Department of Physics, Tianjin University, Tianjin 300354, China

(Received 14 April 2023; accepted 23 June 2023; published 5 July 2023)

We utilize the Boltzmann transport model to investigate the sequential suppression pattern of the $\Upsilon(1S, 2S, 3S)$ states in both small (*p*-Pb) and large (Pb-Pb) collision systems at a center-of-mass energy of $\sqrt{s_{NN}} = 5.02$ TeV. The cold nuclear matter effects occur prior to the formation of bottomonium, which is equivalent for the various bottomonium states $\Upsilon(1S, 2S, 3S)$. The sequential suppression pattern of the bottomonium states is regarded as a manifestation of the hot medium effects, where the bottomonium states experience different levels of color screening and parton inelastic scatterings due to their distinct geometrical sizes and binding energies. Excited states of bottomonium are more susceptible to dissociation due to their smaller binding energies. By incorporating both cold and hot medium effects, the transport model provides a consistent explanation for the experimental observations of bottomonium in both small and large collision systems.

DOI: 10.1103/PhysRevC.108.014901

I. INTRODUCTION

A new deconfined state of matter, consisting of elementary particles such as quarks and gluons [1], is believed to be formed in relativistic heavy-ion collisions. This extremely hot medium is called the quark-gluon plasma (QGP) and has been extensively studied in terms of heavy and light partons [2–9]. Due to their large masses, heavy quarks and quarkonium production can be easily calculated via perturbative quantum chromodynamics (QCD) theories. Heavy quarkonium was first proposed as a probe of the QGP more than 30 years ago by Matsui and Satz [10]. When the medium temperature is sufficiently high, the heavy quark potential is screened by the thermal light partons in the QGP, reducing the binding energy of quarkonium and leading to the dissolution of bound states [11]. Meanwhile, random collisions from thermal partons, including gluon-dissociation [12] and parton quasifree scatterings [13], can also dissociate heavy quarkonium.

Using bottomonium as an example, in heavy-ion collisions at the BNL Relativistic Heavy-Ion Collider (RHIC) and the CERN Large Hadron Collider (LHC), hot medium effects significantly suppress the production of bottomonium, which is characterized by the nuclear modification factor R_{AA}. This factor is defined as the ratio of the bottomonium final production in nucleus-nucleus (*AA*) collisions and the product of the bottomonium yield in proton-proton (*pp*) collisions and the number of binary collisions $N_{\rm coll}$. Hot medium effects differ for different bottomonium states $\Upsilon(1S, 2S, 3S)$ due to their binding energies. A clear sequential suppression pattern has been observed in both *p*-Pb [14] and Pb-Pb [15,16] collisions, where the excited states of bottomonium suffer stronger dissociation in the medium.

Several theoretical models have been developed to study the evolution of heavy quarkonium in relativistic heavy-ion collisions. The rate equation model [7,13], Boltzmann-type transport model [12,17], semiclassical transport model [18,19], and statistical hadronization model [20,21] consider quarkonium dissociation and regeneration from the combination of heavy quark and antiquark in the QGP. The complex potential model based on the Schrödinger equation [22–25] evolves the heavy quarkonium wave function by taking into account in-medium complex potentials, leading to the decoherence of the bottomonium wave package. Open quantum system approaches such as the Lindblad equation [26] and stochastic Schrödinger equation [27] have also been developed to treat heavy quarkonium and quarks as open quantum subsystems in the environment.

In this study, we utilize the Boltzmann transport model to investigate the dynamic evolution of bottomonium in *p*-Pb and Pb-Pb collisions. The decay rate of heavy quarkonium takes into account hot medium effects, such as color screening and gluon dissociation [28]. Furthermore, the initial conditions of the transport equation incorporate cold nuclear matter effects, including shadowing [29] and the Cronin effect [30]. The details of the transport model and the hot medium evolutions are introduced in Sec. II. In Sec. III, theoretical results are compared with the experimental data from *p*-Pb and Pb-Pb collisions. A final conclusion is given in Sec. IV.

II. TRANSPORT MODEL

The transport model is utilized in this study to describe the dynamic evolution of bottomonium in phase space within the quark-gluon plasma. Bottomonium distribution f_Υ in phase space is determined by accounting for bottomonium dissociation and regeneration in the hot medium, and can be expressed

*baoyi.chen@tju.edu.cn

using the equation [31]

$$\left[\cosh(y-\eta)\partial_\tau + \frac{\sinh(y-\eta)}{\tau}\partial_\eta + \boldsymbol{v}_T\cdot\nabla_T\right] f_\Upsilon = -\alpha_\Upsilon f_\Upsilon + \beta_\Upsilon, \quad (1)$$

where $y = 1/2\ln[(E+p_z)/(E-p_z)]$ and $\eta = 1/2\ln[(t+z)/(t-z)]$ are the rapidities in the momentum and coordinate space. $\tau = \sqrt{t^2 - z^2}$ is the proper time. The third term $\mathbf{v}_T\cdot\nabla_T f_\Upsilon$ represents the diffusion of bottomonium in phase space with a constant transverse velocity $\mathbf{v}_T$. Hot medium effects dissociate bottomonium with a rate α_Υ,

$$\alpha_\Upsilon = \frac{1}{2E_T}\int \frac{d^3\mathbf{k}}{(2\pi)^3 2E_g}\sigma_{g\Upsilon}(\mathbf{p},\mathbf{k},T)4F_{g\Upsilon}(\mathbf{p},\mathbf{k})f_g(\mathbf{k},T), \quad (2)$$

where $E_T = \sqrt{m_\Upsilon^2 + p_T^2}$ is the transverse energy of bottomonium, with the mass $m_{\Upsilon(1S,1P,2S,2P,3S)} = (9.46, 9.89, 10.02, 10.25, 10.35)$ GeV taken from Particle Data Group [32]. $\mathbf{k}$ represents the momentum of the gluon. The decay rate of bottomonium induced by gluon dissociation is proportional to the gluon density, f_g, which is assumed to follow a massless Bose distribution. $F_{g\Upsilon}$ is the flux factor in the reaction. The dissociation cross-section of bottomonium in a vacuum can be calculated using the operator-product-expansion method, as described in previous studies [33,34]. The dissociation cross-section formula is expressed as [12]

$$\sigma_{g\Upsilon(1S)\to b\bar{b}}(w) = A_0\frac{(x-1)^{3/2}}{x^5} \quad (3)$$

with the definition $x \equiv w/\epsilon$. $w = p_\Upsilon^\mu k_{g\mu}/m_\Upsilon$ is the energy of gluon in the rest frame of bottomonium moving with a four-momentum p_Υ^μ. The binding energy of $\Upsilon(1S)$, denoted as ϵ, is defined as $\epsilon(0) = 2m_b - m_\Upsilon$ in a vacuum and decreases in a hot medium due to color screening. The bottom quark mass is fixed at $m_b = 5.28$ GeV. To account for the mean color screening effect and neglecting temperature dependence, we approximate the in-medium binding energy of $\Upsilon(1S)$ to be 40% of its vacuum value. The detailed temperature dependence of the decay rate is reflected in the gluon density $f_g(\mathbf{k},T)$ [28]. $A_0 = (2^{11}\pi/27)(m_b^3\epsilon_\Upsilon)^{-1/2}$ is a constant factor.

Bottomonium can also be produced via the combination of bottom and antibottom quarks in the QGP, denoted as β_Υ. This process is proportional to the densities of bottom and antibottom quarks, as well as their coalescence probability which is related to the dissociation rate via detailed balance. The transport model from the TAMU group [13] studies the regeneration contribution in bottomonium nuclear modification factors. It turns out to be smaller than the primordial production for $\Upsilon(1S)$ state. The Langevin plus coalescence model [35] which simulates detailed evolutions of (anti)bottom quarks and their coalescence process, also suggests a small regeneration in bottomonium R_{AA}, while the magnitude of the regeneration depends on the choice of the in-medium heavy quark potential. The Schrödinger equation models [23,24] neglect the regeneration contribution directly when studying bottomonium R_{AA}. Additionally, experimental data on bottomonium $R_{AA}(p_T)$ does not show any evident enhancement or "rise" at low p_T as is observed in the case of J/ψ $R_{AA}(p_T)$. Therefore, even if the regeneration process exists, it is expected to have only a small contribution to the total yield of bottomonium. In this work, we neglect the regeneration contribution in bottomonium production.

The initial distribution of bottomonium in nucleus-nucleus collisions can be approximated as a superposition of effective nucleon-nucleon collisions. The production cross sections of different bottomonium states have been measured in experiments by various collaborations, including CMS [36,37], ATLAS [38], ALICE [39], and LHCb [40–43], at the LHC energies. Using the branching ratios of feed-down processes from the Particle Data Group [32], the direct production cross section of bottomonium before feed-down processes can be extracted as $d\sigma_{\rm direct}(1S,1P,2S,2P,3S)/dy = (37.97, 44.2, 18.27, 37.68, 8.21)$ nb at $\sqrt{s_{NN}} = 5.02$ TeV [23]. To fit the momentum distribution of bottomonium measured by the aforementioned collaborations, the normalized momentum distribution of $\Upsilon(1S)$ can be parametrized with the formula

$$\frac{dN_{pp}^\Upsilon}{2\pi p_T dp_T} = \frac{(n-1)}{\pi(n-2)\langle p_T^2\rangle_{pp}}\left[1 + \frac{p_T^2}{(n-2)\langle p_T^2\rangle_{pp}}\right]^{-n}, \quad (4)$$

where $\langle p_T^2\rangle_{pp} = 80$ (GeV/c)^2 and $n = 2.5$ [23] at the central rapidity of pp collision at $\sqrt{s_{NN}} = 5.02$ TeV. As bottomonium is produced in parton hard scatterings, the initial spatial distribution of $\Upsilon(1S)$ is proportional to the number of nucleon binary collisions $n_{\rm coll}(\mathbf{x}_T)$. In nucleus-nucleus and proton-nucleus collisions, the initial condition of bottomonium is also affected by the cold nuclear matter effect. For example, the Cronin effect can be included via the Gauss smearing method, where $\langle p_T^2\rangle_{pp} + g_{gN}\langle l\rangle$ replaces $\langle p_T^2\rangle_{pp}$ in $dN_{pp}^\Upsilon/(2\pi p_T dp_T)$. Here, $\langle l\rangle$ is the mean path length of partons traveling in the nucleus before the production of $b\bar{b}$ dipole, and $a_{gN} = 0.15$ (GeV/c)^2 [44] is the square of the energy a parton obtains per unit length. Additionally, the nuclear parton density is modified by surrounding nucleons, leading to a shadowing effect that also affects the production of bottomonium in Pb-Pb and p-Pb collisions. The modification factor from the shadowing effect is calculated using the EPS09 package [45], and is multiplied in the initial distributions of bottomonium before the start of the transport equation [44]. Both cold nuclear matter effects can alter the initial distributions of heavy quarks, which will also be reflected in the distributions of open and hidden heavy flavor hadrons [46]. The normalized transverse momentum distributions of excited bottomonium states are assumed to be the same as the ground state due to their similar masses.

The temperature profiles of the hot medium created in p-Pb and Pb-Pb collisions at $\sqrt{s_{NN}} = 5.02$ TeV are determined using a $(2+1)$ dimensional ideal hydrodynamic model. In p-Pb collisions, the maximum initial temperatures of the QGP at forward and backward rapidities are extracted to be $T_c(\mathbf{x}T = 0, b = 0) = 248$ MeV and 289 MeV, respectively, for the most central collisions [22,47–49]. The start time of hydrodynamic equations is $\tau_0 = 0.6$ fm/c, at which point the medium is assumed to have reached local equilibrium. In Pb-Pb collisions,

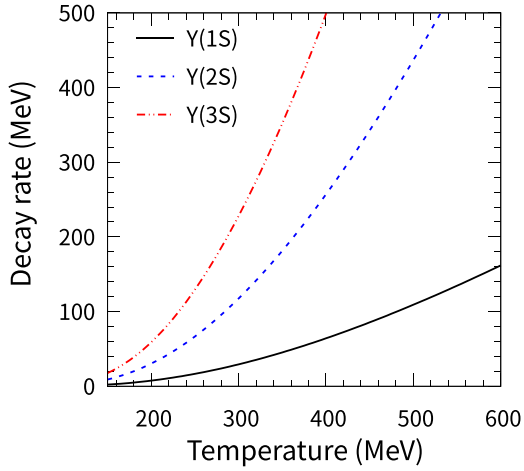

FIG. 1. Decay rates of $\Upsilon(1S, 2S, 3S)$ as a function of temperature in the hot medium. The in-medium binding energy of $\Upsilon(1S)$ is taken to be 40% of the vacuum value to consider the color screening effect. The decay rates of the excited states $\Upsilon(2S, 3S)$ are obtained by the geometry scale with the ground state.

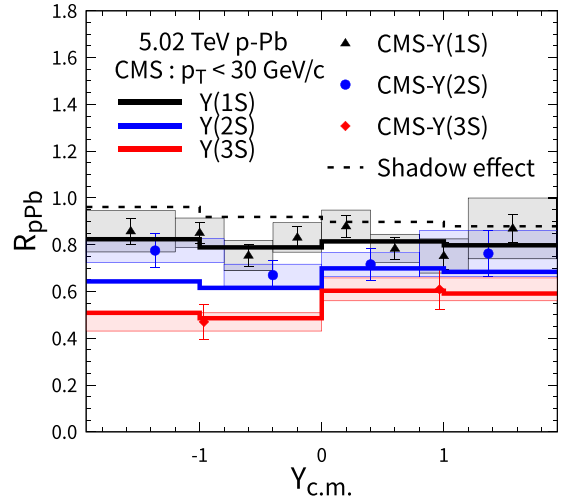

FIG. 2. Nuclear modification factors $R_{p\mathrm{Pb}}$ of $\Upsilon(1S, 2S, 3S)$ in $\sqrt{s_{NN}} = 5.02$ TeV p-Pb collisions. The dashed line includes only cold nuclear matter effects. Solid lines include both cold and hot medium effects. Temperature profiles in forward and backward rapidities are taken in the range $Y_{\mathrm{c.m.}} > 0$ and $Y_{\mathrm{c.m.}} < 0$, respectively. The experimental data are cited from the CMS Collaboration [14].

the maximum initial temperature of the QGP is extracted to be 510 MeV at central rapidity [50]. The critical temperature of the phase transition between QGP and hadronic gas is fixed at $T_c = 165$ MeV for zero baryon chemical potential. From hydrodynamic equations, the lifetimes of the QGP in p-Pb and Pb-Pb collisions are approximately 3 fm/c and 12 fm/c, respectively, for central collisions with $b = 0$. Therefore, bottomonium suffers stronger suppression in Pb-Pb collisions compared with p-Pb collisions, as reflected in their respective RAAs.

III. NUMERICAL RESULTS IN P-PB AND PB-PB COLLISIONS

The dynamical evolutions of bottomonium and the QGP are described by transport and hydrodynamic models, respectively. When calculating the nuclear modification factors of bottomonium, an important ingredient reflecting the interactions between bottomonium and the hot medium is the decay rate of $\Upsilon(1S, 2S, 3S)$. Taking into account both color screening and gluon-dissociation processes, the decay rates of bottomonium states $\Upsilon(1S, 2S, 3S)$ are plotted in Fig. 1. The decay rate of the ground state is calculated using Eq. (2), and the decay rates of excited states are obtained via the geometry scale with the ground state. As we neglect the temperature dependence in the binding energy of bottomonium and assume an effective in-medium binding energy for $\Upsilon(1S)$, the temperature dependence in the decay rates mainly comes from the density of gluons, which increases with temperature.

In p-Pb collisions, the bottomonium nuclear modification factors are plotted as a function of rapidity in Fig. 2 after accounting for both cold and hot nuclear matter effects. The dashed line represents the calculation with only cold nuclear matter effects. The shadowing factor, calculated using the EPS09 package, differs between forward and backward rapidities. Upon considering hot medium dissociation, the nuclear modification factors of $\Upsilon(1S, 2S, 3S)$ are plotted with solid lines in the figure. In the backward rapidity, defined as the direction in which Pb is moving, the antishadowing effect enhances bottomonium production. However, the medium temperatures in the backward rapidities are higher compared to the forward rapidities, resulting in a stronger suppression of bottomonium $R_{p\mathrm{Pb}}$. The combined effects result in similar $R_{p\mathrm{Pb}}$ values for the ground state $\Upsilon(1S)$ in both forward and backward rapidities. The excited states, being more susceptible to hot medium effects, exhibit a greater suppression in the backward rapidities. Additionally, in the pre-equilibrium stage where $\tau < \tau_0$, bottomonium also undergoes hot medium dissociation, with the medium temperature approximated to be the value at $\tau = \tau_0$. The calculation accounts for feed-down processes from higher P states and S states. The contribution of hadronic gas to bottomonium suppression has been neglected due to two reasons. First, at LHC energies, the initial temperatures and lifetimes of the QGP are considerably greater than those of the hadronic phase, especially in nucleus-nucleus collisions, implying that bottomonium suppression is primarily driven by QGP effects. Secondly, our previous research on charmonium suppression at FAIR energies [51] revealed that the hadronic gas could cause an additional ≈10% suppression on J/ψ R_{AA}. This effect would be much less pronounced for bottomonium because of their stronger binding energies and smaller geometry sizes.

The p_T dependence of bottomonium nuclear modification factors is also calculated in Fig. 3. The dashed line includes only cold nuclear matter effects. As experimental data are in the rapidity range $|y| < 1.93$, we use hydrodynamic profiles in forward and backward rapidities, respectively. The corresponding results are plotted as the lower and upper limits of the theoretical bands. $R_{p\mathrm{Pb}}$ increases with transverse momentum due to the shadowing effect and the leakage effect, where

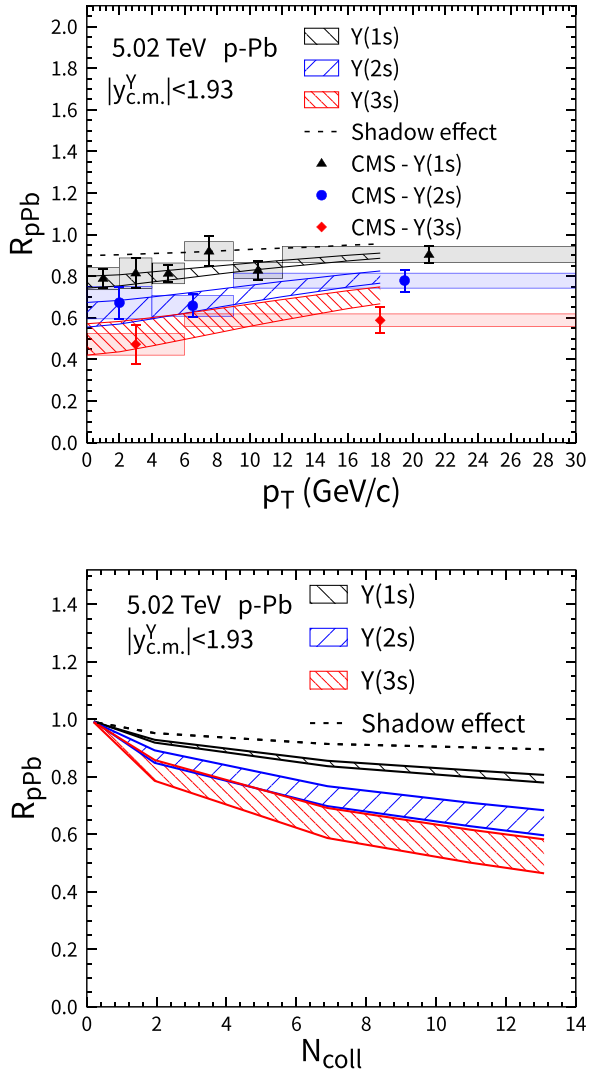

FIG. 3. (Upper panel) $R_{p\mathrm{Pb}}$ of $\Upsilon(1S, 2S, 3S)$ as a function of transverse momentum in $\sqrt{s_{NN}} = 5.02$ TeV p-Pb collisions. The dashed line includes only cold nuclear matter effects. Theoretical bands correspond to the calculations by taking temperature profiles in forward and backward rapidities of p-Pb collisions, respectively. Experimental data are cited from the CMS Collaboration [14]. (Lower panel) Bottomonium $R_{p\mathrm{Pb}}$ as a function of N_{coll}.

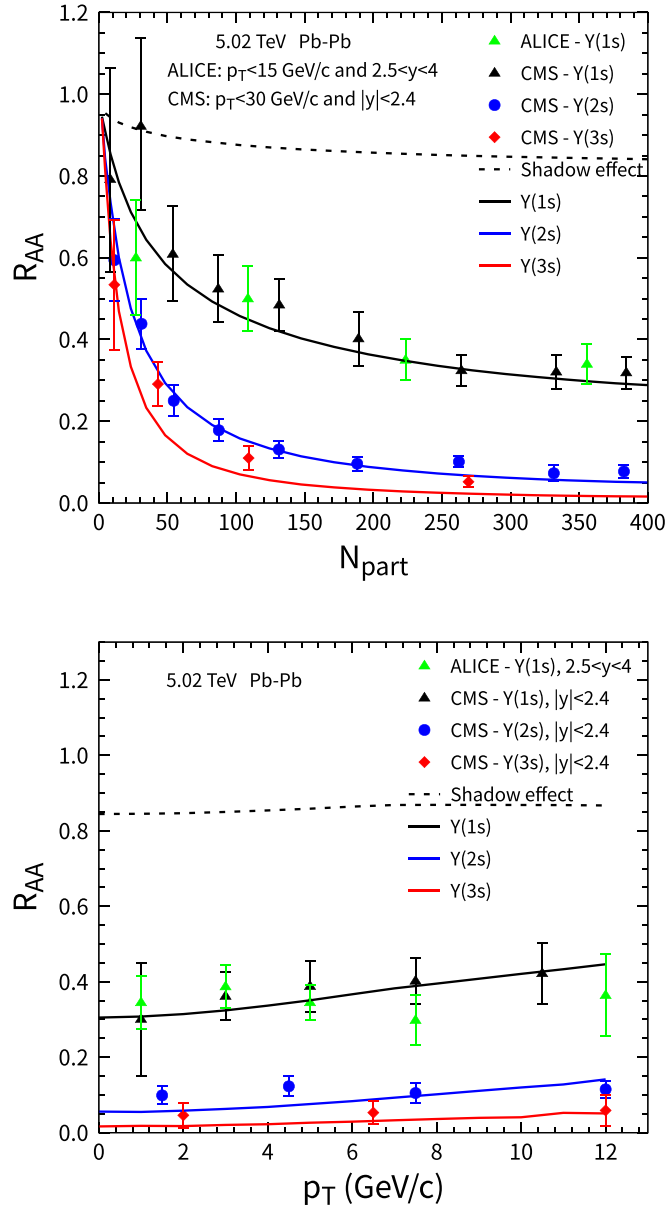

FIG. 4. Bottomonium $R_{AA}(1S, 2S, 3S)$ as a function of N_p (upper panel) and p_T (lower panel) in $\sqrt{s_{NN}} = 5.02$ TeV Pb-Pb collisions. Dashed line includes only cold nuclear matter effects. Different solid lines represent the nuclear modification factors of $\Upsilon(1S, 2S, 3S)$ by taking both cold and hot medium effects and also the feed-down process. The experimental data are cited from CMS [52] and ALICE [16] Collaborations.

bottomonium with larger p_T can escape from the hot medium more quickly. The hot medium effects give rise to differences in $R_{p\mathrm{Pb}}$ for $\Upsilon(1S, 2S, 3S)$. Additionally, we provide calculations for $R_{p\mathrm{Pb}}$ as a function of N_{coll} in Fig. 3, based on the same inputs. The theoretical bands correspond to the calculations with temperature profiles in forward and backward rapidities.

In large collision systems, such as Pb-Pb collisions at $\sqrt{s_{NN}} = 5.02$ TeV, the initial temperatures of the medium can be as high as $\approx 3T_c$. The density of thermal partons is high enough to dissociate most of the ground state bottomonium $\Upsilon(1S)$ and nearly all excited states in central collisions. Only those bottomonium states produced at the edge of the fireball can survive the hot medium. In Fig. 4, we employ the transport model to calculate the bottomonium nuclear modification factors R_{AA} as a function of N_p and p_T. The hot medium effects on $\Upsilon(1S)$ become stronger from peripheral to central collisions. For excited states of bottomonium, their R_{AA} values become close to zero at $N_p \approx 400$ due to significant decay rates. There is a slight increase in the $R_{AA}(p_T)$ of $\Upsilon(1S)$ due to the leakage effect. In the absence of hot medium effects, R_{AA} values for $\Upsilon(1S, 2S, 3S)$ are the same. However, the evident difference between their R_{AA} values indicates strong hot medium suppression in Pb-Pb collisions. The sequential suppression pattern is observed in both p-Pb and Pb-Pb

collisions, which is consistent with other transport models [13] and complex-potential models [23,24].

IV. SUMMARY

In this study, we utilize the Boltzmann transport model to investigate the nuclear modification factors of bottomonium $\Upsilon(1S, 2S, 3S)$ in p-Pb and Pb-Pb collisions at $\sqrt{s_{NN}} = 5.02$ TeV. Cold nuclear matter effects are incorporated in the initial conditions of the transport model. Hot medium effects, such as color screening and gluon dissociation, are taken into account in the decay rate of the ground state, while the decay rates of excited states are obtained via the geometry scale with the ground state. Our theoretical calculations explain well the rapidity and transverse momentum dependence of bottomonium $\Upsilon(1S, 2S, 3S)$ nuclear modification factors in both p-Pb and Pb-Pb collisions, demonstrating a clear pattern of sequential suppression. These consistent theoretical calculations in different collision systems enable the extraction of reliable decay rates of bottomonium states in the quark-gluon plasma.

ACKNOWLEDGMENTS

This work is supported by the National Natural Science Foundation of China (NSFC) under Grant No. 12175165.

[1] A. Bazavov, T. Bhattacharya, M. Cheng, C. DeTar, H. T. Ding, S. Gottlieb, R. Gupta, P. Hegde, U. M. Heller, F. Karsch *et al.*, Phys. Rev. D **85**, 054503 (2012).
[2] A. Andronic, F. Arleo, R. Arnaldi, A. Beraudo, E. Bruna, D. Caffarri, Z. C. del Valle, J. G. Contreras, T. Dahms, A. Dainese *et al.*, Eur. Phys. J. C **76**, 107 (2016).
[3] H. Song, S. A. Bass, U. Heinz, T. Hirano, and C. Shen, Phys. Rev. Lett. **106**, 192301 (2011); **109**, 139904(E) (2012).
[4] P. Braun-Munzinger, V. Koch, T. Schäfer, and J. Stachel, Phys. Rep. **621**, 76 (2016).
[5] M. He, R. J. Fries, and R. Rapp, Phys. Lett. B **735**, 445 (2014).
[6] G. Y. Qin and X. N. Wang, Int. J. Mod. Phys. E **24**, 1530014 (2015).
[7] L. Grandchamp, R. Rapp, and G. E. Brown, Phys. Rev. Lett. **92**, 212301 (2004).
[8] L. Yan, P. Zhuang, and N. Xu, Phys. Rev. Lett. **97**, 232301 (2006).
[9] B. Chen, M. Hu, H. Zhang, and J. Zhao, Phys. Lett. B **802**, 135271 (2020).
[10] T. Matsui and H. Satz, Phys. Lett. B **178**, 416 (1986).
[11] H. Satz, J. Phys. G **32**, R25 (2006).
[12] X. L. Zhu, P. F. Zhuang and N. Xu, Phys. Lett. B **607**, 107 (2005).
[13] X. Du, M. He, and R. Rapp, Phys. Rev. C **96**, 054901 (2017).
[14] A. Tumasyan *et al.* (CMS Collaboration), Phys. Lett. B **835**, 137397 (2022).
[15] A. M. Sirunyan *et al.* (CMS Collaboration), Phys. Rev. Lett. **120**, 142301 (2018).
[16] S. Acharya *et al.* (ALICE Collaboration), Phys. Lett. B **790**, 89 (2019).
[17] Y. Liu, B. Chen, N. Xu, and P. Zhuang, Phys. Lett. B **697**, 32 (2011).
[18] X. Yao and B. Müller, Phys. Rev. D **100**, 014008 (2019).
[19] X. Yao, W. Ke, Y. Xu, S. A. Bass, and B. Müller, J. High Energy Phys. 01 (2021) 046.
[20] A. Andronic, P. Braun-Munzinger, K. Redlich, and J. Stachel, Phys. Lett. B **652**, 259 (2007).
[21] A. Andronic, P. Braun-Munzinger, K. Redlich, and J. Stachel, Nucl. Phys. A **789**, 334 (2007).
[22] L. Wen, X. Du, S. Shi, and B. Chen, Chin. Phys. C **46**, 114102 (2022).
[23] L. Wen and B. Chen, Phys. Lett. B **839**, 137774 (2023).
[24] A. Islam and M. Strickland, J. High Energy Phys. 03 (2021) 235.
[25] A. Islam and M. Strickland, Phys. Lett. B **811**, 135949 (2020).
[26] N. Brambilla, M. Á. Escobedo, M. Strickland, A. Vairo, P. Vander Griend, and J. H. Weber, J. High Energy Phys. 05 (2021) 136.
[27] Y. Akamatsu, M. Asakawa, S. Kajimoto, and A. Rothkopf, J. High Energy Phys. 07 (2018) 029.
[28] B. Chen, Chin. Phys. C **43**, 124101 (2019).
[29] A. H. Mueller and J. W. Qiu, Nucl. Phys. B **268**, 427 (1986).
[30] J. W. Cronin *et al.* (E100 Collaboration), Phys. Rev. D **11**, 3105 (1975).
[31] K. Zhou, N. Xu, Z. Xu, and P. Zhuang, Phys. Rev. C **89**, 054911 (2014).
[32] R. L. Workman *et al.* (Particle Data Group), PTEP **2022**, 083C01 (2022).
[33] M. E. Peskin, Nucl. Phys. B **156**, 365 (1979).
[34] G. Bhanot and M. E. Peskin, Nucl. Phys. B **156**, 391 (1979).
[35] B. Chen and J. Zhao, Phys. Lett. B **772**, 819 (2017).
[36] V. Khachatryan *et al.* (CMS Collaboration), Phys. Rev. D **83**, 112004 (2011).
[37] S. Chatrchyan *et al.* (CMS Collaboration), Phys. Lett. B **727**, 101 (2013).
[38] G. Aad *et al.* (ATLAS Collaboration), Phys. Rev. D **87**, 052004 (2013).
[39] J. Adam *et al.* (ALICE Collaboration), Eur. Phys. J. C **76**, 184 (2016).
[40] R. Aaij *et al.* (LHCb Collaboration), Eur. Phys. J. C **72**, 2025 (2012).
[41] R. Aaij *et al.* (LHCb Collaboration), J. High Energy Phys. 06 (2013) 064.
[42] R. Aaij *et al.* (LHCb Collaboration), Eur. Phys. J. C **74**, 2835 (2014).
[43] R. Aaij *et al.* (LHCb Collaboration), Eur. Phys. J. C **74**, 3092 (2014).
[44] B. Chen, T. Guo, Y. Liu, and P. Zhuang, Phys. Lett. B **765**, 323 (2017).
[45] K. J. Eskola, H. Paukkunen, and C. A. Salgado, J. High Energy Phys. 04 (2009) 065.
[46] C. Zhang, L. Zheng, S. Shi, and Z. W. Lin, arXiv:2210.07767 [nucl-th].
[47] Y. Liu, C. M. Ko, and T. Song, Phys. Lett. B **728**, 437 (2014).
[48] X. Du and R. Rapp, J. High Energy Phys. 03 (2019) 015.
[49] W. Zhao, C. M. Ko, Y. X. Liu, G. Y. Qin, and H. Song, Phys. Rev. Lett. **125**, 072301 (2020).
[50] W. Zhao, H. J. Xu, and H. Song, Eur. Phys. J. C **77**, 645 (2017).
[51] B. Chen, Phys. Rev. C **93**, 044917 (2016).
[52] A. M. Sirunyan *et al.* (CMS Collaboration), Phys. Lett. B **790**, 270 (2019).